Biological control effect of *Trichoderma harzianum* and *Bacillus amyloliquefaciens* on *Neopestalotiopsis rosae* under controlled conditions †

[Efecto del control biológico de *Trichoderma harzianum* y *Bacillus amyloliquefaciens* sobre *Neopestalotiopsis rosae* en condiciones controladas]

Maria Magdalena Cervantes-Zuñiga[1], Kenzy Ivveth Peña-Carrillo[2], Agustín Hernández-Juárez[1], Gabriel Gallegos-Morales[1], Juan Carlos Delgado-Ortiz[1] and Epifanio Castro-del Ángel*[1]

[1]Departamento de Parasitología. Universidad Autónoma Agraria Antonio Narro. Calzada Antonio Narro 1923, C.P. 25315, Saltillo, Coahuila, México.
*[2]Campo experimental General Terán, Instituto Nacional de Investigaciones Forestales Agrícolas y Pecuarias Km 31 Carretera Montemorelos-China, General Terán, Nuevo León, México. E-mail, epifanio.castro@uaaan.edu.mx**
**Corresponding author*

SUMMARY

Background: The strawberry crop (*Fragaria x ananassa*) faces a wide range of fungal phytopathogens that cause various diseases during its phenological cycle, with *Neopestalotiopsis rosae* having a significant impact. **Objective:** To evaluate the biocontrol *in*-vitro of *N. rosae*-induced crown rot by using *Trichoderma harzianum* and *Bacillus amyloliquefaciens* with potential applications in strawberry crops. **Methodology:** The pathogen was isolated from infected plants of the Frontera, Festival and Albion varieties in the state of Michoacán, followed by its purification and morphological and molecular identification. Under laboratory conditions, a strain of *T. harzianum* provided by a phytopathology laboratory was used to perform dual-culture inhibition assays on potato dextrose agar. **Results:** The results showed a percentage of *N. rosae* growth inhibition ranging from 58.94% to 81.63%. Furthermore, in bioassays carried out with *B. amyloliquefaciens*, inhibition percentages were observed, which ranged between 62.50% and 72.87, highlights the potential of both biological agents in the management of this disease. **Implications:** These findings suggest that *Trichoderma harzianum* and *Bacillus amyloliquefaciens* could represent promising components of integrated disease management strategies. Their significant antagonistic activity indicates potential for reducing reliance on synthetic fungicides and supports further investigation under greenhouse and field conditions to validate their efficacy against crown rot caused by *Neopestalotiopsis rosae*. **Conclusion:** The strains of *Trichoderma harzianum* and *Bacillus amyloliquefaciens* demonstrated strong antagonistic activity against *Neopestalotiopsis rosae*, indicating their potential as effective biocontrol agents for managing crown rot in strawberry crops.
Key words: Biocontrol; inhibition; crown rot.

RESUMEN

Introducción: El cultivo de fresa (*Fragaria x ananassa*) se enfrenta a una amplia gama de fitopatógenos fúngicos que causan diversas enfermedades durante su ciclo fenológico, destacando el importante impacto de *Neopestalotiopsis rosae*. **Objetivo:** Evaluar el control biológico *in*-vitro de la pudrición de la corona inducida por *N. rosae* mediante el uso de *Trichoderma harzianum* y *Bacillus amyloliquefaciens*, con potencial aplicación en cultivos de fresa. **Metodología:** El patógeno se aisló de plantas infectadas de las variedades Frontera, Festival y Albion en el estado de Michoacán, y posteriormente se purificó y se identificó morfológica y molecularmente. En condiciones de laboratorio, se utilizó una cepa de *T. harzianum* proporcionada por el laboratorio de fitopatología para realizar ensayos de inhibición en cultivos duales en agar dextrosa-patata. **Resultados:** Los resultados mostraron un porcentaje de inhibición del crecimiento de *N. rosae* que osciló entre el 58.94 % y el 81.63 %. Por otro lado, en los bioensayos realizados con *B. amyloliquefaciens* se observaron porcentajes de inhibición que oscilaron entre el 62.50 % y el 72.87

† *Submitted November 19, 2025 – Accepted March 11, 2026.* http://doi.org/10.56369/tsaes.6709

ISSN: 1870-0462.
ORCID = M.M. Cervantes-Zuñiga: http://orcid.org/0009-0009-7433-2415; **K.I. Peña-Carrillo**: http://orcid.org/0000-0003-0580-6700; **A. Hernández-Juárez**: http://orcid.org/0000-0001-7059-4471; **G. Gallegos-Morales**: http://orcid.org/0000-0001-9041-6904; **J.C. Delgado-Ortiz**: http://orcid.org/0000-0002-2770-7431; **E. Castro-del Ángel**: http://orcid.org/0000-0002-5534-1262

%, lo que pone de relieve el potencial de ambos agentes biológicos en el manejo de esta enfermedad. **Implicaciones:** Estos hallazgos sugieren que *Trichoderma harzianum* y *Bacillus amyloliquefaciens* podrían representar componentes prometedores en estrategias integradas de manejo de enfermedades. Su significativa actividad antagónica indica potencial para reducir la dependencia de fungicidas sintéticos y justifica la realización de más investigaciones en condiciones de invernadero y de campo para validar su eficacia contra la pudrición de la corona causada por *Neopestalotiopsis rosae*. **Conclusión:** Las cepas de *Trichoderma harzianum* como *Bacillus amyloliquefaciens* demostraron una fuerte actividad antagónica contra *Neopestalotiopsis rosae*, lo que indica su potencial como agentes de control biológico eficaces para gestionar la pudrición de la corona en los cultivos de fresas.
Palabras clave: Control biológico; inhibición; pudrición de la corona.

INTRODUCTION

Strawberries (*Fragaria* × *ananassa* Duch.) are among the most widely consumed and valued fruits worldwide (Ahmad et al., 2017; Álvarez-Medina et al., 2017; Arroyo and Hernández, 2021). This crop holds significant economic importance for Mexico, which currently ranks third globally as a strawberry producer and exporter, with a production value exceeding 15.4 billion pesos (SIAP, 2024). However, strawberry production is severely affected by various diseases, particularly crown rot, caused by the fungus *Neopestalotiopsis* sp. (Sun *et al*., 2021). This disease damages the upper parts of the plant, including the crown and stolons, leading to yield losses exceeding 70% (Baggio *et al*., 2021; Essa *et al*., 2018; Kaur *et al*., 2022).

Over the past decade, agricultural systems have relied heavily on agrochemical use for the control of weeds, insects, and plant pathogens. However, this dependency has resulted in severe environmental and health consequences, including biodiversity loss and soil degradation (Mitra *et al*., 2022). Furthermore, the increasing cost of pesticides—particularly in resource-limited regions and consumer demand for pesticide-free products have driven the search for sustainable alternatives.

Currently, management of crown rot primarily relies on the use of chemical fungicides; however, their excessive application poses serious environmental and human health risks (Darapanit *et al*., 2021; Saldaña, 2021). Therefore, it is necessary to develop environmentally friendly and safer alternatives for disease control.

Biological control represents a viable alternative to chemical methods and is defined as the use of living organisms, including viruses, to suppress pest populations such as pathogens, insects, mites, or weeds, thereby providing agricultural and ecological benefits, microbial biological control agents act through multiple mechanisms, including competition for nutrients and space, production of antifungal metabolites, and induction of systemic resistance in plants (Stenberg *et al*., 2021).

Among the most effective biocontrol microorganisms, *Trichoderma harzianum* and *Bacillus amyloliquefaciens* have shown significant potential in controlling various fungal diseases affecting agricultural crops (Chun *et al*., 2018; Lee *et al*., 2017; Wang *et al*., 2021; Zalila-Kolsi *et al*., 2022; Yan *et al*., 2020).

In this context, the present study aimed to evaluate the biocontrol *in*-vitro efficacy of *T. harzianum* and *B. amyloliquefaciens* against strawberry crown rot caused by *Neopestalotiopsis* sp. The findings of this study are expected to contribute to the development of environmentally friendly and sustainable disease management strategies that enhance strawberry production and profitability while minimizing ecological impact and human health risks.

MATERIALS AND METHODS

Sample collection

Sampling was conducted in July 2023 from adult strawberry plants (*Fragaria* × *ananassa* Duch.) of several cultivars grown in nurseries and commercial fields located in the municipalities of Maravatío, Irimbo, and Epitacio Huerta in the state of Michoacán.

The first sampling took place on July 9 and 10, 2023, in the municipality of Irimbo, where samples were collected from two different sites of the ‘Frontera’ cultivar. Both symptomatic and asymptomatic plants were sampled. The sampling strategy consisted of excluding three edge rows from each plot and leaving the first and last two meters of each sampled row uncollected. Starting from that point, three samples were taken every two meters along each row, resulting in a total of 73 samples per site.

The second sampling was conducted on July 11 and 12, 2023, in the municipality of Maravatío, following the same sampling design as the previous one. Two sites planted with the ‘Festival’ cultivar were sampled, with three samples collected from each point (initial, middle, and final section), totaling 73 samples per site. The third sampling was carried out on July 13, 2023, in the municipality of Epitacio Huerta, using the same methodology described above. However, in this

location, sampling focused on dead plants and those showing severe symptoms. A total of 19 samples were collected from site 1 and 40 from site 2, yielding 59 samples for this municipality.

Once the samples were collected, they were placed in paper bags and transported to the Phytopathology Laboratory for processing. The plant material was subsequently washed and disinfected prior to pathogen isolation.

Isolating the plant pathogen

Isolation of the phytopathogenic fungus was performed at the Phytopathology Laboratory of the Department of Parasitology, Universidad Autónoma Agraria Antonio Narro, this procedure consisted of placing four fragments from the crown region of each plant sample—collected from the municipality of Epitacio Huerta (sites 1 and 2)—onto previously prepared PDA (Potato Dextrose Agar) medium in Petri dishes. Two Petri dishes were prepared per sample, resulting in a total of 38 dishes for site 1 and 80 dishes for site 2. Samples from the second municipality, Irimbo (sites 3 and 4), were processed using the same protocol. Two Petri dishes were prepared per sample, yielding a total of 146 dishes for each site.

Finally, plant samples from the municipality of Maravatío (sites 5 and 6) were processed in the same manner, with two Petri dishes prepared per sample, for a total of 146 dishes per site. All inoculated dishes were incubated at 26 °C for three days, after which the growth of the target fungus was verified. Subsequently, two isolates were obtained from each culture. Purification of the fungal isolates was achieved through monoconidial culture techniques. Morphological characterization at the genus level was carried out using the taxonomic keys proposed by Maharachchikumbura et al. (2014).

Molecular identification

DNA extraction was performed using the DNeasy Plant kit (QIAGEN®) per the manufacturer's instructions. The quantity and quality of the extracted DNA was measured with the NanoDrop 2000, equipment. Then, molecular identification was conducted by amplifying the universal ITSs regions with the primers ITS1 (5'-TCC GTA GGT GAA CCT GCG G-3') and ITS4 (5'-TCC TCC GCT TAT TGA TAT GC-3') (White et al., 1990). The gene *elongation factor 1-alpha* (EF-1α) with primers EF1-728F (5'-CAT CGA GAA GTT CGA GAA GG-3'), EF-2 (5'-GGA RGT ACC AGT SAT CAT GTT-3'), (Carbone and Kohn, 1999).

For ITSs regions PCR reactions were carried on in 25 µl of reaction containing: 1x buffer, 3.5 mM MgCl2, 10 mM dNTPs, 2.5 µM of each primer, and 1U Taq platinum (Invitrogen®). The amplification protocol involved one cycle at 94 ºC for 5 min., 35 cycles at 94 ºC for 30 sec, 60 ºC for 45 sec, 72 ºC for 1.5 min, and a final extension at 72 ºC for 8 min. For the elongation factor (tef1α), PCR amplification was performed using a specific program of 35 cycles, consisting of 30 seconds at 95°C, 30 seconds at 48°C, and 1 minute at 72°C. PCR products were visualized on 2 % agarose gels and sent to sequence for purification and sequencing via Sanger technology.

Bioinformatics

The chromatogram files (. ab1) corresponding to the forward and reverse reads were inspected and edited in SnapGene. The quality of each chromatogram was evaluated based on the definition and separation of the peaks. Strands showing weak signal intensity, overlapping peaks, or ambiguous base calls ("N") were trimmed to retain only high-quality segments. Then, samples that contained high-quality forward and reverse reads were assembled using SnapGene's Assemble Contigs tool, with manual verification of the overlap between complementary regions. A consensus sequence was generated for each sample and exported in FASTA format.

To strengthen the phylogenetic framework of the sequences obtained in this study, reference sequences corresponding to the same molecular markers were selected based on the phylogeny reported by Acosta-González et al. (2025). The species *Pestalotiopsis trachicarpicola* and *Pseudopestalotiopsis cocos* (Shi et al., 2024) were included as outgroup taxa. Separate alignments were performed for each molecular marker, including the samples of interest, reference taxa, and outgroup sequences, using the algorithm MUSCLE implemented in SnapGene. Individual gene alignments were subsequently concatenated in MEGA 12 (Kumar et al., 2024) using the Data → Open Multiple Files (concatenate) command. The resulting alignment contained all loci merged into a single continuous sequence per taxon, and the concatenated dataset was exported in FASTA format for downstream analyses.

Phylogenetic reconstruction was conducted using IQ-TREE v3 (Nguyen *et al*., 2015; Minh *et al*., 2020). The concatenated alignment (concatenated_alignments.fas) included high quality sequences of only five strains, it was analyzed under the maximum-likelihood (ML) framework with ModelFinder Plus (Kalyaanamoorthy *et al*., 2017) to automatically select the best-fit nucleotide substitution model. The exact command executed on command line was: iqtree3 -s concatenated_alignments.fas -m MFP -bb 1000 -alrt 1000. Node support was evaluated using 1000 ultrafast bootstrap replicates (UFBoot; Hoang *et al*., 2018) and 1000 SH-aLRT replicates (Guindon *et*

al., 2010), both implemented in IQ-TREE 3. UFBoot provides a rapid approximation of conventional bootstrap proportions, whereas SH-aLRT offers complementary likelihood-ratio-based support values. The resulting maximum-likelihood tree was visualized in Fig Tree software.

Although multi-partition analyses can accommodate gene-specific substitution patterns, an unpartitioned model was selected for this study to avoid potential over-parameterization given the moderate size of the dataset and the overall similarity in evolutionary rates and base compositions among loci. Preliminary tests in MEGA 12 indicated congruent topologies (supplementary file) between separate- and combined-gene analyses, supporting the suitability of a single, global model for maximum-likelihood inference in IQ-TREE 3.

In vitro inhibitory activity against *Neopestalotiopsis rosae*

The trial was conducted in April 2024 and consisted of an in vitro confrontation between the phytopathogen *Neopestalotiopsis rosae* (The 17 strains were selected considering their growth rate, colony color, and acervulus abundance) and the antagonistic agents *Bacillus amyloliquefaciens* and *Trichoderma harzianum*. For this purpose, 5 mm diameter agar discs with active mycelium of the phytopathogen grown for seven days were placed in the center of Petri dishes containing potato dextrose agar (PDA) culture medium.

In the case of *B. amyloliquefaciens*, the bacterial strain was inoculated using a bacteriological loop in the directions corresponding to the four cardinal points of the Petri dish, at 3 cm between inoculation points. 10 replicates were established for each strain of *N. rosae*, and the plates were incubated for seven days, until the control (without antagonist) completely covered the surface of the medium.

The confrontation between *T. harzianum* and the phytopathogen was carried out by placing discs of mycelium from both fungi facing each other at a distance of 3 cm. Ten replicates were also performed for each strain of *N. rosae.* Mycelial growth measurements were taken daily using a digital flexometer, and the radial growth of the phytopathogen in the presence of each antagonist strain was determined. The percentage of radial growth inhibition (PI) was calculated using the control growth as a reference, using the following equation:

$$PI = 100 - [(Cr * 100)/Rp]$$

where: PI = percentage of growth inhibition of the phytopathogen; Cr = radial growth of the mycelium of the phytopathogen in confrontation; and Rp = total radius of the Petri dish (Castillo-Reyes *et al*., 2015).

A completely random design was used, differences in inhibition were determined by Tukey's mean test at a significance level of 0.05, using SAS version 9.0 software.

RESULTS AND DISCUSSION

Morphological identification

Seventeen fungal isolates were obtained from symptomatic strawberry plants and identified at the genus level as *Neopestalotiopsis*, based on the taxonomic keys proposed by Maharachchikumbura *et al*. (2014) (Figure 1). En la Tabla 1 se reportan los accesos de las secuencias depositadas en el GEnBank

After two days of incubation at 26 °C, colonies exhibited a nearly rosette-like morphology, while some isolates showed circular and cottony growth on PDA medium, the aerial mycelium appeared white and velvety. As growth progressed, colonies expanded radially from the center, resembling flower petals, with irregular margins and a faint yellow coloration; some isolates displayed a pale pink hue on the reverse side of the Petri dish. Between days 7 and 10 of incubation, depending on the isolate, colonies reached full coverage of the medium surface.

At later growth stages, small black, shiny, globose, and viscous structures appeared on the mycelial surface, identified as acervuli. The hyphae were branched but aseptate. Conidia were fusiform, straight or slightly curved, with four septa, and measured 23–26 µm in length. Each conidium contained three to six cells, with the central cells being brown and the terminal cells nearly hyaline. Among the pigmented cells, the first two were dark brown, whereas the third exhibited a lighter brown coloration.

Based on these morphological characteristics, the pathogen was identified as a species belonging to the genus *Neopestalotiopsis* sp., in accordance with Maharachchikumbura *et al*. (2014).

Molecular identification

According to the molecular identification based on sequences of ITSs regions and elongation factor 1-alpha, the strains of study correspond to the species *Neopestalotiopsis rosae*, in the phylogenetic tree they were together clustered. With respect to beta-tubulin sequences, unfortunately, they were very poor quality and impossible to use.

Table 1. Molecular identification of *Neopestalotiopsis rosae* strains using ITS and EF-1α markers and their GenBank accession.

ITS	EF-1α	Isolation location	GenBank ITS access	GenBank EF-1α access
1	18	Epitacio Huerta	PZ091918	PX516886
2	19	Epitacio Huerta	PZ091919	PX516887
3	20	Epitacio Huerta	PZ091920	PX516889
4	21	Epitacio Huerta	PZ091921	PX516890
5	-	Epitacio Huerta	-	-
6	22	Epitacio Huerta	-	-
7	-	Irimbo	PZ091922	PX516885
8	-	Irimbo	-	-
9	-	Irimbo	-	-
10	-	Irimbo	-	-
11	-	Irimbo	PZ091923	-
12	-	Irimbo	-	-
13	23	Maravatío	PZ091924	PX516884
14	24	Maravatío	PZ091925	PX516888
15	25	Maravatío	PZ091926	PX516891
16	26	Maravatío	PZ091927	PX516892
17	-	Maravatío	-	-

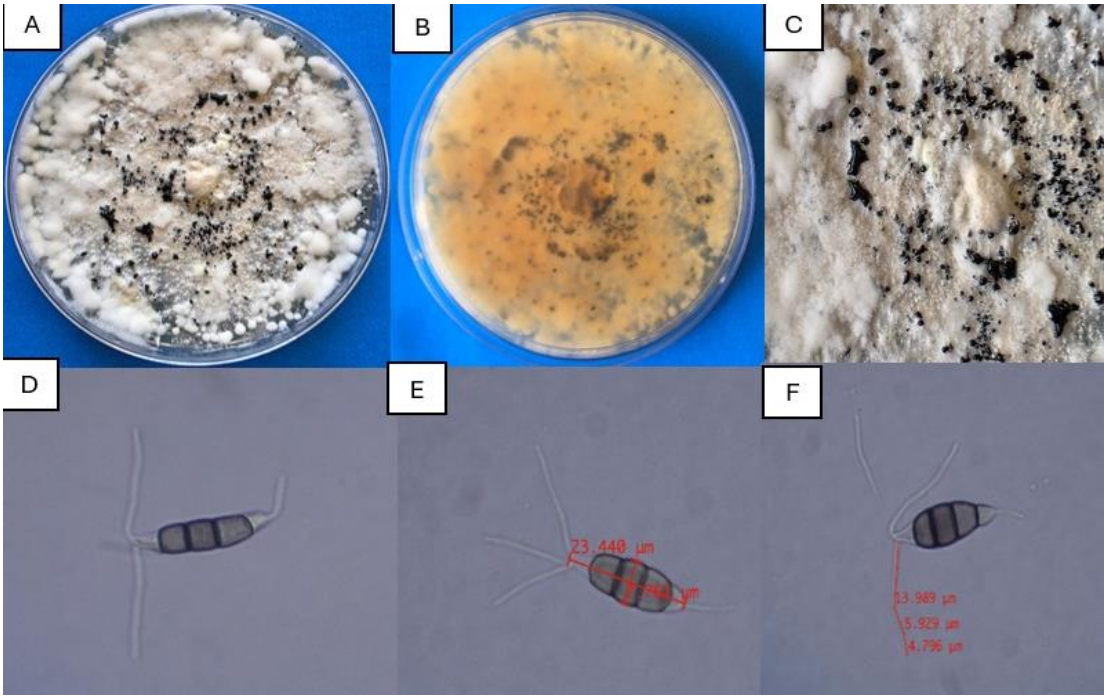

Figure 1. (A and B) White mycelium, PDA front and back of the colony cream-colored; C) Black acervuli; D) Conidia of *Neopestalotiopsis*; (E and F) subcylindrical ellipsoid conidial structures with 4-5 septa.

Conidia bore two to three non-branched, hyaline apical appendages measuring 17–22 µm in length, and one to two basal appendages measuring 5–7 µm. The acervuli were black, globose, and viscous, with conidia adhered to their surface.

It is important to highlight that phylogenetic analyses show that there is a need to increase the number of genes for phylogenetic studies or to turn to genomic scale analyses, to try to solve the phylogeny of the genus *Neopestalotiopsis;* not all species of *Neopestalotiopsis* were monophyletic, e.g. *N. clavispora,* which is a closed related species to *N. rosae*.

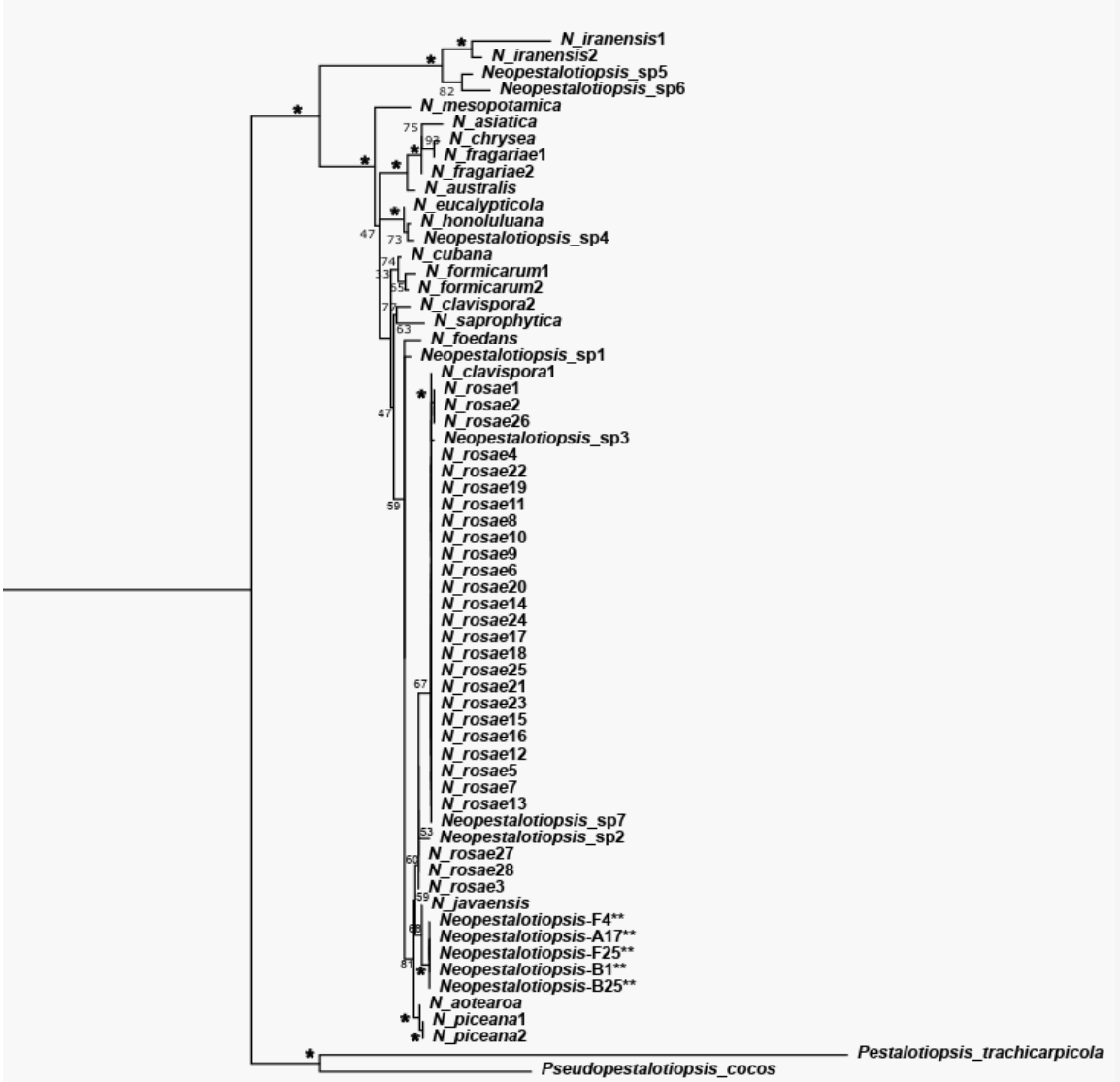

Figure 2. Maximum-likelihood phylogeny of *Neopestalotiopsis* based on ITS and EF-1α. The concatenated tree includes isolates obtained in this study (marked "") and those reported by Acosta-González *et al.* (2025). *Pseudopestalotiopsis coco* and *Pestalotiopsis trachycarpicola* were used as outgroups. * Bootstrap percentages ≥ 90 % are shown at nodes.**

In vitro inhibitory activity of *Trichoderma harzianum* against *Neopestalotiopsis rosae*

Dual confrontation: a significant effect ($P < 0.05$) was observed in the study of mycelial growth of *Neopestalotiopsis rosae* colonies against *Trichoderma harzianum* strains, which showed reduced growth compared to the control for some strains (Figure 2 and Figure 3). This may be due to the fact that *Trichoderma* has different mechanisms of action that give it the potential to control phytopathogens, including: competition for space, favored by the growth rate of the isolates; mycoparasitism, involving chemotrophic processes that promote recognition, adhesion, coiling, and lytic activity of chitinases and cellulases, mainly (Stange *et al*. 2023; Infante *et al*. 2009).

Figure 2. Direct confrontation between *Neopestalotiopsis rosae* and *Trichoderma harzianum* strain (which obtained the highest percentage of inhibition).

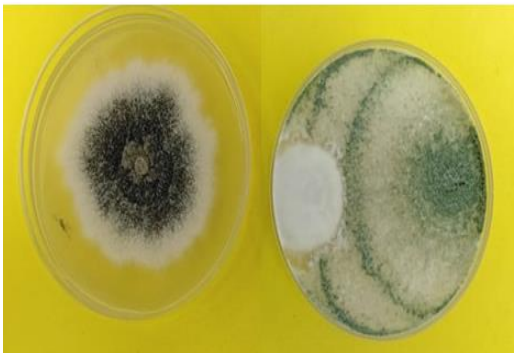

Figure 3. Direct confrontation between *Neopestalotiopsis rosae* and *Trichoderma harzianum* strain (which obtained a lower percentage of inhibition).

Other authors also mention that *Trichoderma* can have hook-shaped structures, coils, or appressoria around the host that allow it to penetrate the pathogen and degrade it (Chen *et al*., 2024; Güçlü and Özer 2022). This mechanism is accompanied by the secretion of enzymes such as chitinase to degrade the pathogen's cell wall (Stange *et al*., 2023). In particular, the antagonistic effect of *Trichoderma* is due to the action of enzymes, which can degrade the cell wall, chitin, proteins, and lipids (Kredics *et al*., 2024). In addition, it produces secondary metabolites such as polyketides, non-ribosomal peptides, terpenoids, pyrones, antibiotics, among others, which function as growth inhibitors; it can also act as a mycoparasite, competing for space or nutrients (Chen *et al*., 2025; Guzmán-Guzmán *et al*., 2025).

The contact time between antagonist and pathogen was 3 days, which is consistent with the findings of other authors who obtained similar results and determined that *Trichoderma* spp. and various pathogens come into contact one to three days after the dual culture test is established (Stange *et al*., 2023) (Table 2). To evaluate mycoparasitism, the scale of (Bell *et al*., 1982) was used.

During the confrontation, rapid growth of the *T. harzianum* strain was observed on both the front and back of the Petri dish, with inhibition percentages ranging from 58.94% for the IRI C33 strain to a maximum of 81.63% for the IRI D43 strain. It should be noted that some of the *Neopestalotiopsis* strains did not behave uniformly in terms of acervulus production, as some of them produced acervuli 6 days after the bioassay was established, unlike other strains, where this occurred 12 to 13 days later.

It was also observed that some strains did not exhibit 100% mycoparasitism. This may be due to genetic variability between strains, even when they are of the same species and collected from the same site.

Table 2. Percentage of antagonistic capacity of *Trichoderma harzianum* against strains of *Neopestalotiopsis rosae.*

STRAIN	Mycelium diameter (CM)			Inhibition ratio
	Control	Inhibition ratio		
	Neopestalotiopsis rosae	*T. harzianum*	*Neopestalotiopsis rossae*	
Neopestalotiopsis rosae. E.H A11	2.23	4.67	1.49	66.98 bc
Neopestalotiopsis rosae. E.H A17	2.18	4.63	1.53	70.36 bac
Neopestalotiopsis rosae. E.H B25	2.3	4.51	1.54	67.08 bac
Neopestalotiopsis rosae. E.H B1	2.24	4.67	1.49	66.70 bc
Neopestalotiopsis rosae. IRI C9	2.11	4.54	1.49	71.01 bac
Neopestalotiopsis rosae. IRI C33	2.23	4.89	1.31	58.94 c
Neopestalotiopsis rosae. IRI D43	2.27	4.56	1.6	81.63 a
Neopestalotiopsis rosae. IRI D3	2.22	4.33	0.92	76.19 ba
Neopestalotiopsis rosae. Mar E8	2.22	4.33	1.56	70.39 bca
Neopestalotiopsis rosae. Mar F25	2.33	4.35	1.35	66.73 bc
Neopestalotiopsis rosae. Mar F4	2.22	4.41	1.38	71.37 bac
Neopestalotiopsis rosae. E.H A1	2.14	4.51	1.39	64.92 bc
Neopestalotiopsis rosae. E.H B22	2.06	4.54	1.38	68.04 bac
Neopestalotiopsis rosae. IRI C31	2.11	4.6	1.33	63.21 bc
Neopestalotiopsis rosae. IRI D12	2.22	4.79	1.07	66.17 bc
Neopestalotiopsis rosae. Mar E30	2.21	4.53	1.35	61.31 c
Neopestalotiopsis rosae. Mar F18	2.19	4.6	1.37	62.72 bc

In vitro* inhibitory activity of *Bacillus amyloliquefaciens* against *Neopestalotiopsis rosae

Some strains showed high levels of growth inhibition when confronted with *B. amyloliquefaciens*, indicating the high potential of this bacterial species as an antagonist of this pathogen (Figure 4 and Figure 5). The percentage of inhibition among microorganisms evaluated *in vitro* shows that *Neopestalotiopsis* strains were inhibited in a range from 62.50 % (strain IRI D3) to a maximum of 72.88 % (strain IRI C9) (Table 3). This is because *Bacillus* is a beneficial bacterium, and during its growth, it produces a series of metabolites that can inhibit the activity of fungi and bacteria. Most previous studies have focused on the direct antimicrobial characteristics of *Bacillus* or the antifungal substances it produces (Gharsallah *et al*., 2025; Hernández-Rodríguez *et al*., 2024).

Figure 4. Direct confrontation of *Neopestalotiopsis rosae* with *Bacillus amyloliquefaciens* strain (IRI C9), which obtained the highest percentage of inhibition.

Figure 5. Direct confrontation of *Neopestalotiopsis rosae* with *Bacillus amyloliquefaciens* strain (IRI D3), which obtained a lower percentage of inhibition.

Among these secondary metabolites, lipopeptides are widely studied as antimicrobial agents and are classified into three main groups according to their structure: iturins, surfactins, and fengicins. Studies have shown that the inhibitory effects of lipopeptides on pathogens are mainly manifested in the suppression of mycelial growth and impact spore germination (Ding *et al*., 2025). Some research mentions that the suppression of various plant diseases by *B. amyloliquefaciens* involves mechanisms that include competitive action, antibiotics, induction of plant resistance (ISR), and promotion of plant growth, antibiotics are a fundamental mechanism in the control of plant diseases through the secretion of lipopeptide substances, polyketide compounds, and antimicrobial proteins (Saiyam *et al*., 2024; Zhang *et al*., 2024).

The wide range of metabolites produced by bacteria of the genus *Bacillus*, which can act against fungi, including antibiotics, lipopeptides, lytic enzymes, and siderophores (Marnani *et al*., 2025). Other authors mention that the bacterium *B. amyloliquefaciens* stimulates resistance to infections by *Botrytis pelargonii* and *Alternaria alternata*. (Kazerooni, 2021) report that *B. amyloliquefaciens* inhibits 85% of the growth of *Fusarium*, isolated from ginseng (*Panax ginseng* Meyer) cultivation. Some studies mention that *B. amyloliquefaciens* is characterized by its antifungal activity against some pathogenic fungi such as *Alternaria citri, Botryosphaeria* sp. and *Colletotrichum gloeosporioides* (Zalila-Kolsi *et al*., 2022). It has been reported that the iturine lipopeptide family is responsible for the antagonism of *B. amyloliquefaciens* against this fungus, similarly, *B. amyloliquefaciens* has a general bacteriostatic effect on *Alternaria hydrophila*, and the main bacteriostatic substance is an extracellular product (Hanif *et al*., 2019).

The contact time between the antagonist and the pathogen was three days. After that time, in most confrontations, the *Neopestalotiopsis* strain remained static in the presence of the *Bacillus amyloliquefaciens* bacterium. It should be noted that some *Neopestalotiopsis* strains presented acervuli three days after the bioassay was established. This may be because the *Neopestalotiopsis* fungus has the ability to produce a variety of bioactive compounds, which can be used as defense mechanisms against competitors such as *Trichoderma*, *Bacillus*, and other pathogenic fungi. These compounds can interfere with the enzymatic activities of these competing organisms, in addition to altering the cellular structure of pathogenic bacteria and fungi.

Table 3. Percentage of antagonistic capacity of *Bacillus amyloliquefaciens* against strains of *Neopestalotiopsis rosae*.

Strain	Mycelium diameter (CM)		Percentage Inhibition
	Control *Neopestalotiopsis rosae*	Inhibition *Bacillus amyloliquefaciens*	
Neopestalotiopsis sp. E.H A1	3.95	1.12	71.58 ba
Neopestalotiopsis sp. E.H B22	3.94	1.40	64.63 edc
Neopestalotiopsis sp. IRI C31	3.96	1.25	68.52 ebdac
Neopestalotiopsis sp. IRI D12	3.55	1.48	68.93 ebdac
Neopestalotiopsis sp. Mar E30	3.72	1.20	67.70 ebdac
Neopestalotiopsis sp. Mar F18	3.97	1.26	68.37 ebdac
Neopestalotiopsis sp. E.H A11	3.86	1.16	70.03 bdac
Neopestalotiopsis sp. E.H A17	4.10	1.33	65.16 ebdc
Neopestalotiopsis sp. E.H B1	4.23	1.29	69.46 bdac
Neopestalotiopsis sp. E.H B25	4.04	1.19	70.46 bac
Neopestalotiopsis sp. IRI C9	3.90	1.06	72.87 a
Neopestalotiopsis sp. IRI C33	3.09	1.11	65.16 ebdc
Neopestalotiopsis sp. IRI D43	3.84	1.23	63.58 edf
Neopestalotiopsis sp. IRI D3	3.83	1.23	62.50 ef
Neopestalotiopsis sp. Mar E8	3.87	1.21	68.97 bac
Neopestalotiopsis sp. Mar F25	3.86	1.2	70.76 bac
Neopestalotiopsis sp. Mar F4	3.86	1.21	66.74 ebdac

CONCLUSIONS

The results obtained *in vitro* trials demonstrated that both *Bacillus amyloliquefaciens* and *Trichoderma harzianum* are highly effective in controlling *Neopestalotiopsis rosae*, as evidenced by the high percentages of inhibition of the phytopathogen´s mycelial growth. These results suggest that both biocontrol agents have significant potential for use as sustainable alternatives in the management of diseases caused by *N. rosae*, thereby contributing to the reduction in the use of synthetic fungicides and the development of more environmentally friendly biological control strategies.

Funding. Thanks to the Universidad Autónoma Agraria Antonio Narro for funding this project (38111 425101001 2136) and to the Laboratorio de Plagas Cuarantenadas at Campo Experimental General Terán for the assistance provided in the molecular study.

Conflict of interests. The authors declare no conflict of interests.

Compliance with ethical standards. It does not apply.

Data availability. Data is available at a reasonable request to the corresponding author.

Author contribution statement (CRediT). M.M. Cervantes-Zuñiga – Conceptualization, supervision, writing -review and editing. **K. I. Peña-Carrillo** – Conceptualization, supervision, writing -review and editing., **A. Hernández-Juárez** – Conceptualization, supervision, writing -review and editing. **G. Gallegos-Morales** –Conceptualization, supervision, writing -review and editing. **J. C. Delgado-Ortiz** – Conceptualization, supervision, writing -review and editing. **E. Castro-del Ángel** – Conceptualization, supervision, funding acquisition, writing -review and editing.

REFERENCES

Acosta-González, U., García-García, G., Silva-Rojas, H.V., Peres, N.A., Marin, M.V., Rebello, C.S., Fuentes-Aragón, D., Leyva-Mir, S.G. and Rebollar-Alviter, Á., 2025. Molecular, cultural and pathogenic characterization of *Neopestalotiopsis rosae* from strawberry in Mexico. https://doi.org/10.31219/osf.io/wz7ms_v1

Ahmad, H., Sajjid, M., Hayat, S., Ullah, R., Ali, M., Jamal, A. and Ali, J., 2017. Growth, yield and fruit quality of strawberry (*Fragaria ananassa* Duch.) under different phosphorus levels. *Research in Agriculture*, 2(2), pp. 19–26. http://dx.doi.org/10.22158/ra.v2n2p19

Álvarez-Medina, A., Silva-Rojas, H. V., Leyva-Mir, S. G., Marbán-Mendoza, N. and Rebollar-Alviter, Á., 2017. Resistencia de *Botrytis cinerea* de strawberry (*Fragaria* × *ananassa* Duch.) a fungicidas en Michoacán, México. *Agrociencia*, 51(7), pp. 783–798.

Arroyo, C.A.J. and Hernández, F.A.A., 2021. Competitiveness of the Mexican strawberry in the US market from 1992 to 2017. *Ciencia y Tecnología Agropecuaria*, 22(1). https://doi.org/10.21930/rcta.vol22

Baggio, J.S., Forcelini, B.B., Wang, N.Y., Ruschel, R.G., Mertely, J.C. and Peres, N.A., 2021. Outbreak of leaf spot and fruit rot in Florida strawberry caused by *Neopestalotiopsis* spp. *Plant Disease*, 105(2), pp. 305–315. https://doi.org/10.1094/PDIS-06-20-1290-RE

Bell, D.K., Wells, H.D. and Markham, C.R., 1982. In vitro antagonism of *Trichoderma* species against six fungal plant pathogens. *Phytopathology*, 72(4), pp. 379–382. https://doi.org/10.1094/Phyto-72-379

Carbone, I. and Kohn, L.M., 1999. A method for designing primer sets for speciation studies in filamentous ascomycetes. *Mycologia*, 91(3), pp. 553–556. https://doi.org/10.2307/3761358

Castillo-Reyes, F., Hernández-Castillo, F.D., Gallegos-Morales, G., Flores-Olivas, A., Rodríguez-Herrera, R. and Aguilar, C. N. (2015). Efectividad *in vitro* de *Bacillus* y polifenoles de plantas nativas de México sobre *Rhizoctonia solani*. *Revista Mexicana de Ciencias Agrícolas*, 6(3), pp. 549-562.

Chen, S., Daly, P., Anjago, W.M., Wang, R., Zhao, Y., Wen, X., Zhou, D., Deng, S., Lin, X., Voglmeir, J., Cai, F., Shen, Q., Druzhinina, I.S. and Wei, L., 2024. Genus-wide analysis of *Trichoderma* antagonism toward *Pythium* and *Globisporangium* plant pathogens and the contribution of cellulases to the antagonism. *Applied and Environmental Microbiology*, 90(9), e00681-24. https://doi.org/10.1128/aem.00681-24

Chen, X., Lu, Y., Liu, X., Gu, Y. and Li, F., 2025. *Trichoderma*: dual roles in biocontrol and plant growth promotion. *Microorganisms*, 13(8), 1840. https://doi.org/10.3390/microorganisms13081840

Chun, J., Yang, H. E. and Kim, D. H., 2018. Identification of a novel partitivirus of *Trichoderma harzianum* NFCF319 and evidence for the related antifungal activity. *Frontiers in Plant Science*, 9, 1699. https://doi.org/10.3389/fpls.2018.01699

Darapanit, A., Boonyuen, N., Leesutthiphonchai, W., Nuankaew, S. and Piasai, O., 2021. Identification, pathogenicity and effects of plant extracts on *Neopestalotiopsis* and *Pseudopestalotiopsis* causing fruit diseases. *Scientific Reports*, 11(1), 22606. https://doi.org/10.1038/s41598-021-02113-5

Ding, N., Dong, H. and Ongena, M., 2025. Bacterial cyclic lipopeptides as triggers of plant immunity and systemic resistance against pathogens. *Plants*, 14(17), 2644. https://doi.org/10.3390/plants14172644

Essa, T.A., Kamel, S.M., Ismail, A.M. and El-Ganainy, S., 2018. Characterization and chemical control of *Neopestalotiopsis rosae*, the causal agent of strawberry root and crown rot in Egypt. Egyptian Journal of *Phytopathology*, 46(1), pp. 1–19. https://doi.org/10.21608/ejp.2018.87411

Gharsallah, H., Cheffi, M., Mallek, R., Massoudi, A., Omri, N., Triki, M.A., Öztop, M.H. and Zarai, Z., 2025. Antifungal potential of *Bacillus* strains: implications for biocontrol strategies in food safety and sustainable agriculture. *Frontiers in Microbiology*, 16, 1615252. https://doi.org/10.3389/fmicb.2025.1615252

Güçlü, T. and Özer, N., 2022. *Trichoderma harzianum* antagonistic activity and competition for seed colonization against seedborne pathogenic fungi of sunflower. *Letters in Applied Microbiology*, 74(6), pp. 1027–1035. https://doi.org/10.1111/lam.13698

Guindon, S., Dufayard, J.F., Lefort, V., Anisimova, M., Hordijk, W. and Gascuel, O., 2010. New algorithms and methods to estimate maximum-likelihood phylogenies: Assessing the performance of PhyML 3.0, *Systematic Biology*, 59(3), pp. 307–321. https://doi.org/10.1093/sysbio/syq010

Guzmán-Guzmán, P., Etesami, H. and Santoyo, G., 2025. *Trichoderma*: a multifunctional agent in plant health and microbiome interactions. *BMC Microbiology*, 25(1), 434. https://doi.org/10.1186/s12866-025-04158-2

Hanif, A., Zhang, F., Li, P., Li, C., Xu, Y., Zubair, M., Zhang, M., Jia, D., Zhao, X., Liang, J., Majid, T., Yan, J., Farzand, A., Wu, H., Gu, Q. and Gao, X., 2019. Fengycin produced by *Bacillus amyloliquefaciens* FZB42 inhibits *Fusarium graminearum* growth and mycotoxin biosynthesis. *Toxins*, 11(5), 295. https://doi.org/10.3390/toxins11050295

Hernández-Rodríguez, M., Jasso-de Rodríguez, D., Hernández-Castillo, F.D., Moggio, I., Arias, E., Valenzuela-Soto, J.H. and Flores-Olivas, A., 2024. The rhizobacterium *Bacillus amyloliquefaciens* MHR24 has biocontrol ability against fungal phytopathogens and promotes growth in *Arabidopsis thaliana*. *Microorganisms*, 12(11), 2380. https://doi.org/10.3390/microorganisms12112380

Hoang, D.T., Chernomor, O., von Haeseler, A., Minh, B.Q. and Vinh, L.S., 2018. UFBoot2: improving the ultrafast bootstrap approximation. *Molecular Biology and Evolution*, 35(2), pp. 518–522. https://doi.org/10.1093/molbev/msx281

Infante, D., Martínez, B., González, N. and Reyes, Y., 2009. Mecanismos de acción de *Trichoderma* frente a hongos fitopatógenos. *Revista de Protección Vegetal*, 24(1), pp. 14–21.

Kaur, H., Gelain, J., Marin, M.V., Peres, N.A. and Schnabel, G., 2022. Development of a molecular tool for identification of a new *Neopestalotiopsis* species associated with disease outbreaks on strawberry. *Plant Disease*, 107(5), pp. 1544–1549. https://doi.org/10.1094/PDIS-09-22-2117-RE

Kazerooni, E.A., Maharachchikumbura, S.S., Al-Sadi, A. M., Kang, S. M., Yun, B.W. and Lee, I.J., 2021. Biocontrol potential of *Bacillus amyloliquefaciens* against *Botrytis pelargonii* and *Alternaria alternata* on *Capsicum annuum*. *Journal of Fungi*, 7(6), 472. https://doi.org/10.3390/jof7060472

Kalyaanamoorthy, S., Minh, B.Q., Wong, T.K.F., von Haeseler, A. and Jermiin, L.S., 2017. ModelFinder: fast model selection for accurate phylogenetic estimates. Nature Methods, 14, pp. 587–589. https://doi.org/10.1038/nmeth.4285

Kredics, L., Büchner, R., Balázs, D., Allaga, H., Kedves, O., Racić, G., Varga, A., Nagy, V.D., Vágvölgyi, C. and Sipos, G., 2024. Recent advances in the use of *Trichoderma*-containing multicomponent microbial inoculants for pathogen control and plant growth promotion. *World Journal of Microbiology and Biotechnology*, 40(5), 162. https://doi.org/10.1007/s11274-024-03965-5

Kumar, S., Stecher, G., Suleski, M., Sanderford, M., Sharma, S. and Tamura, K., 2024. Molecular evolutionary genetics analysis version 12 for adaptive and green computing. *Molecular Biology and Evolution*, 41(12), pp. 1–9. https://doi.org/10.1093/molbev/msae263

Lee, T., Park, D., Kim, K., Lim, S.M., Yu, N.H., Kim, S., Kim, H., Jung, K.S., Jang, J.Y., Park, J., Ham, H., Lee, S., Hong, S.K. and Kim, J.C., 2017. Characterization of *Bacillus amyloliquefaciens* DA12 showing potent antifungal activity against mycotoxigenic *Fusarium* species. *The Plant Pathology Journal*, 33(5), pp. 499–507. https://doi.org/10.5423/PPJ.FT.06.2017.0126

Maharachchikumbura, S.S., Hyde, K.D., Groenewald, J.Z., Xu, J. and Crous, P.W., 2014. *Pestalotiopsis* revisited. *Studies in Mycology*, 79(1), pp. 121–186. https://doi.org/10.1016/j.simyco.2014.09.005

Marnani, M.A., Madani, M. and Shakib, P., 2026. Extraction and characterization of iturin A as a key factor in the antagonism of *Bacillus amyloliquefaciens* M13RW01 toward pathogenic fungi. Recent Patents on Biotechnology, 20(1), pp. 155–165. https://doi.org/10.2174/0118722083352297250326041149

Minh, B.Q., Schmidt, H.A., Chernomor, O., Schrempf, D., Woodhams, M.D., von Haeseler, A. and Lanfear, R., 2020. IQ-TREE 2: new models and efficient methods for phylogenetic inference in the genomic era. *Molecular Biology and Evolution*, 37(5), pp. 1530–1534. https://doi.org/10.1093/molbev/msaa015

Mitra, B., Chowdhury, A.R., Dey, P., Hazra, K.K., Sinha, A.K., Hossain, A. and Meena, R.S., 2022. Use of agrochemicals in agriculture: alarming issues and solutions. In: Input Use Efficiency for Food and Environmental Security. *Springer Nature Singapore*, pp. 85–122. https://doi.org/10.1007/978-981-16-5199-1_4

Nguyen, L.T., Schmidt, H.A., von Haeseler, A. and Minh, B.Q., 2015. IQ-TREE: a fast and effective stochastic algorithm for estimating maximum-likelihood phylogenies. *Molecular Biology and Evolution*, 32(1), pp. 268–274. https://doi.org/10.1093/molbev/msu300

Saiyam, D., Dubey, A., Malla, M. A. and Kumar, A., 2024. Lipopeptides from *Bacillus*: unveiling biotechnological prospects—sources, properties, and diverse applications. *Brazilian Journal of Microbiology*, 55(1), pp. 281–295. https://doi.org/10.1007/s42770-023-01228-3

Saldaña Jaramillo, J., 2021. Control de hongos patógenos con *Bacillus subtilis* y *Trichoderma koningiopsis* en un cultivo de strawberry en condiciones de campo. Tesis de maestría. Instituto Politécnico Nacional, México.

Servicio de Información Agroalimentaria y Pesquera., 2024. Producción agrícola por cultivo: fresa (*Fragaria* × *ananassa*). Secretaría de Agricultura y Desarrollo Rural, Ciudad de México, México. SIAP. Disponible en: https://www.gob.mx/siap

Stange, P., Seidl, S., Karl, T. and Benz, J.P., 2023. Evaluation of *Trichoderma* isolates as biocontrol measure against *Claviceps purpurea*. *European Journal of Plant Pathology*, 167(4), pp. 651–675. https://doi.org/10.1007/s10658-023-02716-w

Stenberg, J.A., Sundh, I., Becher, P.G., Björkman, C., Dubey, M., Egan, P.A., Friberg, H., Gil, J.F., Jensen, D.F., Jonsson, M., Karlsson, M., Khalil, S., Ninkovic, V., Rehermann, G., Vetukuri, R. R. and Viketoft, M., 2021. When is it biological control? A framework of definitions, mechanisms, and classifications. *Journal of Pest Science*, 94(3), pp. 665–676. https://doi.org/10.1007/s10340-021-01354-7

Sun, Q., Harishchandra, D., Jia, J., Zuo, Q., Zhang, G., Wang, Q., Yan, J., Zhang, W. and Li, X., 2021. Role of *Neopestalotiopsis rosae* in causing root rot of strawberry in Beijing, China. *Crop Protection*, 147, 105710. https://doi.org/10.1016/j.cropro.2021.105710

Shi, J., Li, B., Wang, S., Zhang, W., Shang, M., Wang, Y. and Liu, B., 2024. Occurrence of *Neopestalotiopsis clavispora* causing apple leaf spot in China. *Agronomy*, 14(8), 1658. https://doi.org/10.3390/agronomy14081658

Wang, X.Y., Xu, T.T., Sun, L.J., Cen, R.H., Su, S., Yang, X.Q., Yang, Y. and Ding, Z.T., 2021. The chemical diversity, the attractant, anti-acetylcholinesterase, and antifungal activities of metabolites from biocontrol *Trichoderma harzianum* uncovered by OSMAC strategy. *Bioorganic Chemistry*, 114, 105148. https://doi.org/10.1016/j.bioorg.2021.105148

White, T.J., Bruns, T., Lee, S. and Taylor, J., 1990. Amplification and direct sequencing of fungal ribosomal RNA genes for phylogenetics. In: PCR Protocols: A Guide to Methods and Applications. Academic Press, pp. 315–322.

Yan, F., Li, C., Ye, X., Lian, Y., Wu, Y. and Wang, X., 2020. Antifungal activity of lipopeptides from *Bacillus amyloliquefaciens* MG3 against *Colletotrichum gloeosporioides* in loquat fruits. *Biological Control*, 146, 104281. https://doi.org/10.1016/j.biocontrol.2020.104281

Zalila-Kolsi, I., Kessentini, S., Tounsi, S. and Jamoussi, K., 2022. Optimization of *Bacillus amyloliquefaciens* BLB369 culture medium by response surface methodology for low cost production of antifungal activity. *Microorganisms*, 10(4), 830. https://doi.org/10.3390/microorganisms10040830

Zhang, R., Yu, J., Yang, L., Qiao, J., Qi, Z., Yu, M., Du, Y., Song, T., Cao, H., Pan, X., Liu, Y. and Liu, Y., 2024. Surfactins and iturins produced by *Bacillus velezensis* Jt84 strain synergistically contribute to the biocontrol of rice false smut. *Agronomy*, 14(10), 2204. https://doi.org/10.3390/agronomy14102204

Supplementary Table.
Accession numbers corresponding to the taxa used to complement the phylogenetic reconstruction of species within the genus *Neopestalotiopsis*.

Taxa	GenBank accession number	
	ITS	tefl
N_aotearoa	KM199369	KM199526
N_asiatica	JX398983	JX399049
N_australis	KM199348	KM199537
N_chrysea	JX398986	JX399052
N_clavispora 1	KU096879	KU096881
N_cubana	KM199347	KM199521
N_eucalypticola	KM199376	KM199551
N_foedans	JX398987	JX399053
N_formicarum1	KM199344	KM199519
N_formicarum2	KM199358	KM199517
N_fragariae1	ON651145	ON685196
N_fragariae2	ON651146	ON685197
N_honoluluana	KM199364	KM199548
N_iranensis1	KM074045	KM074053
N_iranensis2	KM074048	KM074051
N_javaensis	KM199357	KM199543
N_mesopotamica	KM074047	KM074054
N_clavispora2	JX398979	JX399045
N_piceana1	KM199368	KM199527
N_piceana2	KM199372	KM199529
N_rosae1	OR999336	PP003942
N_rosae2	MK895142	MK903334
N_rosae3	MN385718	MN268532
N_rosae4	KM199359	KM199523
N_rosae5	OR999325	PP003931
N_rosae6	OR999327	PP003933
N_rosae7	OR999328	PP003934
N_rosae8	OR999329	PP003935
N_rosae9	OR999330	PP003936
N_rosae10	OR999331	PP003937
N_rosae11	OR999332	PP003938
N_rosae12	OR999333	PP003939
N_rosae13	OR999334	PP003940
N_rosae14	OR999335	PP003941
N_rosae15	OR999337	PP003943
N_rosae16	OR999338	PP003944
N_rosae17	OR999339	PP003945
N_rosae18	OR999340	PP003946
N_rosae19	OR999341	PP003947
N_rosae20	OR999342	PP003948
N_rosae21	OR999343	PP003949
N_rosae22	OR999344	PP003950
N_rosae23	OR999345	PP003951
N_rosae24	OR999346	PP003952
N_rosae25	OR999347	PP003953
N_rosae26	KY688075	KY688074
N_rosae27	MN385719	MN268533
N_rosae28	MN495972	MN968328
N_saprophytica	JX398982	JX399048
Neopestalotiopsis_sp1	KX894994	KX895211
Neopestalotiopsis_sp2	MN238829	MN704864
Neopestalotiopsis_sp3	OR999326	PP003932
Neopestalotiopsis_sp4	KM199350	KM199550

Taxa	GenBank accession number	
	ITS	tefl
Neopestalotiopsis_sp5	PP150438	PP157636
Neopestalotiopsis_sp6	PP150439	PP157637
Neopestalotiopsis_sp7	MK895144	MK903336
Pestalotiopsis_trachicarpicola	JX399002	JX399066
Pseudopestalotiopsis_cocos	MH855069	KM199553

Supplementary Figure. Maximum-likelihood phylogenetic tree inferred from the ITS gene sequences. The tree was reconstructed using IQ-TREE v3 under the best-fit substitution model selected by ModelFinder Plus (Kalyaanamoorthy et al., 2017).

Supplementary Figure. Maximum-likelihood phylogenetic tree inferred from the tef1 gene sequences.0.03 The tree was reconstructed using IQ-TREE v3 under the best-fit substitution model selected by ModelFinder Plus (Kalyaanamoorthy et al., 2017).